Biochemical and Biophysical Research Communications 404 (2011) 453–457

Contents lists available at ScienceDirect

Biochemical and Biophysical Research Communications

journal homepage: www.elsevier.com/locate/ybbrc

Induction of *c-fos* transcription in the medaka brain (*Oryzias latipes*) in response to mating stimuli

Teruhiro Okuyama [a], Yuji Suehiro [a], Haruka Imada [a], Atsuko Shimada [a], Kiyoshi Naruse [b], Hiroyuki Takeda [a], Takeo Kubo [a], Hideaki Takeuchi [a,*]

[a] Department of Biological Sciences, Graduate School of Science, The University of Tokyo, Bunkyo-ku, Tokyo 113-0033, Japan
[b] Laboratory of BioResource, National Institute for Basic Biology, Myodaiji, Okazaki, Aichi 444-8585, Japan

ARTICLE INFO

Article history:
Received 19 November 2010
Available online 5 December 2010

Keywords:
c-fos
Mating behavior
Teleost
Medaka
Telencephalon

ABSTRACT

Immediate-early genes (IEGs) are useful for mapping active brain regions in various vertebrates. Here we identified a *c-fos* homologue gene in medaka and demonstrated that the amounts of *c-fos* transcripts and proteins in the medaka brain increased in relation to an artificially evoked seizure, suggesting that the homologue gene has the characteristics of IEGs, which are used as markers of neural activity. Next, quantitative reverse-transcription-polymerase chain reaction revealed that female mating behaviors upregulated *c-fos* transcription in some brain regions including the telencephalon, optic tectum, and cerebellum. In addition, we performed *in situ* hybridization with a *c-fos* intron probe to detect the de novo synthesis of *c-fos* transcripts and confirmed induction of *c-fos* transcription in these brain regions after mating. This is the first report of IEG induction in response to mating stimuli in teleost fish. Our results indicated that *c-fos* expression was induced in response to behavioral stimuli in the medaka brain and that medaka *c-fos* could be a useful marker of neural activity.

1. Introduction

The medaka (*Oryzias latipes*) is a freshwater teleost fish native to East Asia that has long been an ornamental fish in Japan. Medaka exhibit various social interactions, such as schooling behavior [1,2], aggressive behavior [3], and a female mating preference for large males [4]. The medaka mating behaviors, for example, comprise a series of behavioral steps. First, the male medaka approaches the female and swims underneath her [5,6]. Then the male swims rapidly in a small circle, which is called a "quick circle". If the female is receptive to the male courtship display, the fish copulate by crossing their cloaca. As the medaka is a model organism for molecular genetics [7], functional analysis of the neural circuits involved in social interactions using advanced genetic methods will contribute to a better understanding of the neural/molecular basis underlying vertebrate social interactions.

Immediate-early gene (IEG) expression is induced in neurons by stimuli naturally associated with behaviors and the localization of IEG expression is a useful marker of neural activity. Based on IEG expression, brain regions that are active in response to (social) behavioral stimuli have been identified in vertebrate brains, such as rodents [8], songbirds, [9], and anurans [10]. Brain regions associated with mating behavior have been successfully mapped. For example, mating in rodent significantly increases the number of Fos-immunoreactive neurons in several brain regions, including the medial preoptic area, bed nucleus of the stria terminalis, medial amygdala, hypothalamic ventromedial nucleus, subparafascicular thalamic nucleus, and midbrain central tegmental field [8,11]. Although IEG mapping studies have been extensively performed in mammalian and avian model systems, similar analyses in fish have been limited to a few studies in teleost fish [12–14]. Here we identified a medaka *c-fos* homologue gene and demonstrated that IEG expression was induced in response to mating stimuli.

2. Materials and methods

2.1. Fish

Medaka fish (*O. latipes*, dr-R strain) were maintained in like groups in plastic aquariums (12 cm × 13 cm × 19 cm). Sexually mature male and female adult medaka fish (more than 3 months after hatching) were used for the cDNA cloning, real-time PCR, Western blotting, and *in situ* hybridization studies.

2.2. Mating condition

The adult female and male medaka fish were separated by two tanks overnight, prior to mating (Fig. 4A). The next morning, the male and female were placed together in a single tank and then the pair began to exhibit mating behavior within 5-min. We confirmed that the females exhibited normal mating behavior,

* Corresponding author. Fax: +81 3 5841 4448.
E-mail address: takeuchi@biol.s.u-tokyo.ac.jp (H. Takeuchi).

0006-291X/$ - see front matter © 2010 Elsevier Inc. All rights reserved.
doi:10.1016/j.bbrc.2010.11.143

including crossing and spawning, and the males exhibited normal mating behavior, including approach, courtship, and ejaculation.

2.3. Quantification of the c-fos transcript

Real-time RT-PCR was performed with Light Cycler-DNA master hybridization probes (Roche) according to the manufacturer's protocol, using gene-specific primers (c-fos; and 5′-TTCAGAAGAAGCG CTCAAGGA-3′ and 5′-AAGAGCAAGCCTTGGATGAAG-3′; actin; 5′-C TGTCTTTCCCTCCATCGTT-3′ and 5′-TGAGGTAGTCTGTAAGGTCG-3′). The amount of *c-fos* transcript was normalized with that of actin. No significant difference was detected in the levels of actin transcripts [15] between pentylenetetrazole (PTZ) -exposed, control medium-exposed, and mating-stimulated medaka.

2.4. In situ hybridization

In situ hybridization of tissue sections was performed as described previously with some modifications [15,16]. Paraffin-embedded coronal brain sections (10-μm thick) were fixed in 4% paraformaldehyde in phosphate buffered saline, pretreated, and hybridized with digoxigenin (DIG)-labeled riboprobes. The *c-fos* first intron fragment was amplified with forward primer: 5′-GT AAATTGAAACGACGATTGCTTAGATG-3′ and reverse primer: 5′-CT GAGAGAAAGAGGGAGGG-3′ using a genome DNA BAC plasmid ola1-200A07 (National BioResource Project) as a template. The DIG-labeled riboprobes were synthesized by T7 or SP6 polymerase with a DIG labeling mix (Roche) from a template containing the *c-fos* first intron fragment. After stringent washes, DIG-labeled riboprobes were detected immunocytochemically with peroxidase-conjugated anti-DIG antibody (1:500; Roche) and TSA Biotin System (Perkin Elmer). Sense probes were used as negative controls and the signals were confirmed to be antisense probe-specific in every experiment. Micrographs of section *in situ* hybridization were taken using a BX50 optical microscope (Olympus). Intensity and brightness of the micrographs were processed with Photoshop software (Adobe, San Jose, CA).

2.5. Western blotting

Protein detection was performed with antibodies against c-fos (anti-c-Fos (K-25): sc-253, Santa Cruz Biotechnology Inc., Santa Cruz, CA) and β-actin (mouse anti-actin monoclonal antibody: MAB1501, Chemicon International). Blots were simultaneously incubated with differentially labeled species-specific secondary antibodies after transfer to membranes [anti-rabbit IgG conjugated with HRP and anti-mouse IgG conjugated with HRP].

3. Results

3.1. Medaka c-fos homologue has characteristics of an immediate-early gene

To search for active regions in the medaka brain, we focused on the *c-fos* gene as an IEG that is transiently expressed in active neuronal cells. We found an exon encoding a putative medaka *c-fos* homologue in the medaka genome database and isolated a full-length cDNA using the 5′-and 3′-rapid amplification of the cDNA ends (RACE) method (Genbank No. AB572350). The open reading frame encoded 364 amino acids, which had the highest identities (57% and 60%) with fos homologues in mouse (Genbank No. NM_010234) and zebrafish (Genbank No. NM_205569), respectively, which have IEG characteristics [17,18]. First we examined whether medaka *c-fos* homologue also has IEG characteristics. In some rodents, the expression of IEGs is induced in brain regions corresponding to sites of seizure initiation [19,20]. Exposure to a common convulsant agent (PTZ; a GABA-A receptor antagonist) induces stereotyped seizure behavior and leads to *c-fos* expression in zebrafish [18].

First, quantitative reverse transcription-polymerase chain reaction (qRT-PCR) was used to demonstrate the temporal induction of *c-fos* transcription following PTZ exposure. Medaka fish were transferred from a tank with normal medium to a tank with PTZ (10-mM)-containing medium. Adult medaka was exposed to PTZ for 0, 10, 20, 30, 40, 60, and 90 min and then total RNA from the whole brain was isolated. We also isolated total RNA from medaka that was transferred to normal bathing medium as controls. An increase in *c-fos* transcripts levels was detected within minutes after initiating the stimulus, peaked around 30 min, and returned to basal levels within 60 min (Fig. 1A). Next, we analyzed c-Fos protein expression levels using Western blotting with an anti-c-Fos antibody, whose epitope mapped within an internal region of c-Fos of human origin (datasheet from Santa Cruz Biotechnology). Total protein from the whole brain in which adult medaka fish were exposed to 10-mM PTZ for 0, 30,60, 90, 120, and 150 min was isolated. Western blot analysis using the medaka brain lysate showed a major band at approximately 63 kDa (Supplementary Fig. S1), whose molecular weight is consistent with that of homolog proteins in mouse and zebrafish [21,22]. Further, using normal IgG as the primary antibody instead of the c-Fos antibody, we confirmed that there was no nonspecific labeling at bands of the same size as the c-Fos immunoreactive protein (Fig. 1B, lower panel). In medaka exposed to PTZ for 60 min, the level of c-Fos immunoreactive protein was significantly upregulated in comparison with medaka exposed to PTZ for 30 min or untreated control medaka (Fig. 1B, upper panel). Taken together, we concluded that the medaka *c-fos* homologue had IEG activity.

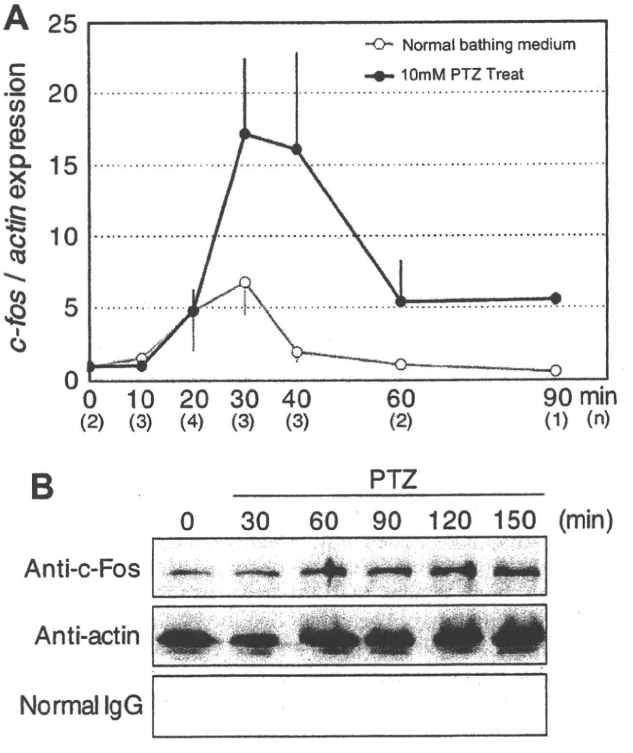

Fig. 1. Immediate early induction of medaka c-fos homologue in the whole brain in response to seizure. (A) The time course of the *c-fos* transcript level revealed by qRT-PCR. All data are shown as the means ± SEM. (B) The time course of the amount of c-Fos protein using Western blotting analysis.

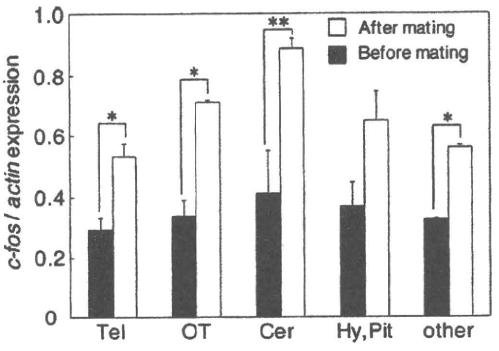

Fig. 2. Mating stimulation induced *c-fos* transcription in various regions of the female brain. Comparison of *c-fos* mRNA expression investigated by qRT-PCR in The telencephalon (Tel), optic tectum (OT), cerebellum (Cer), hypothalamus and pituitary gland (Hy, Pit), and other regions. (*$P < 0.05$; **$P < 0.01$; Student's *t*-test) All data are shown as the means ± SEM.

3.2. Mating stimulation induced c-fos transcription in various brain regions of the female brain

To examine whether *c-fos* expression is induced in response to behavioral stimuli, we investigated changes in *c-fos* expression in the female brain during mating behavior. The female brains were sampled 30 min after mating behavior, because *c-fos* transcripts were sufficiently increased within 30 min of neural stimulation (Fig. 1).

First, we quantitatively analyzed *c-fos* transcripts in the female brain using qRT-PCR. We compared the amount of *c-fos* transcripts in five regions of the female brain before and after mating: the telencephalon, optic tectum, cerebellum, hypothalamus and pituitary gland, and other regions that mainly contained the medulla oblongata and the anterior part of the spinal cord. (Fig. 2). Mating behavior significantly increased *c-fos* transcripts in the telencephalon, optic tectum, cerebellum, and other regions. In the hypothalamus with pituitary gland, the level of *c-fos* transcripts after mating tended to be higher than that before mating, although the difference was not significant. These results suggest that mating stimulation induced *c-fos* transcription in very broad areas of the female brain.

3.3. Detection of localization of c-fos expression in response to mating stimulation using in situ hybridization

To detect only the immediate early induction of *c-fos* transcription (the de novo synthesis of *c-fos* transcripts), we performed *in situ* hybridization using a probe corresponding to the first intron sequence of the *c-fos* gene, which generally improves the temporal and spatial resolution of IEG mapping [23]. To examine whether immature *c-fos* transcripts can be detected using the *c-fos* intron probe, we prepared paraffin sections of brain using medaka exposed to 10-mM PTZ for 30 min, and then performed *in situ* hybridization. Dot-like signals were detected in the telencephalon and hypothalamus (Fig. 3A and Supplementary Fig. S2). In addition, very few dot-like signals were observed in medaka without PTZ treatment. Therefore, we concluded that the de novo synthesis of *c-fos* transcripts could be detected using *in situ* hybridization method with a *c-fos* intron probe.

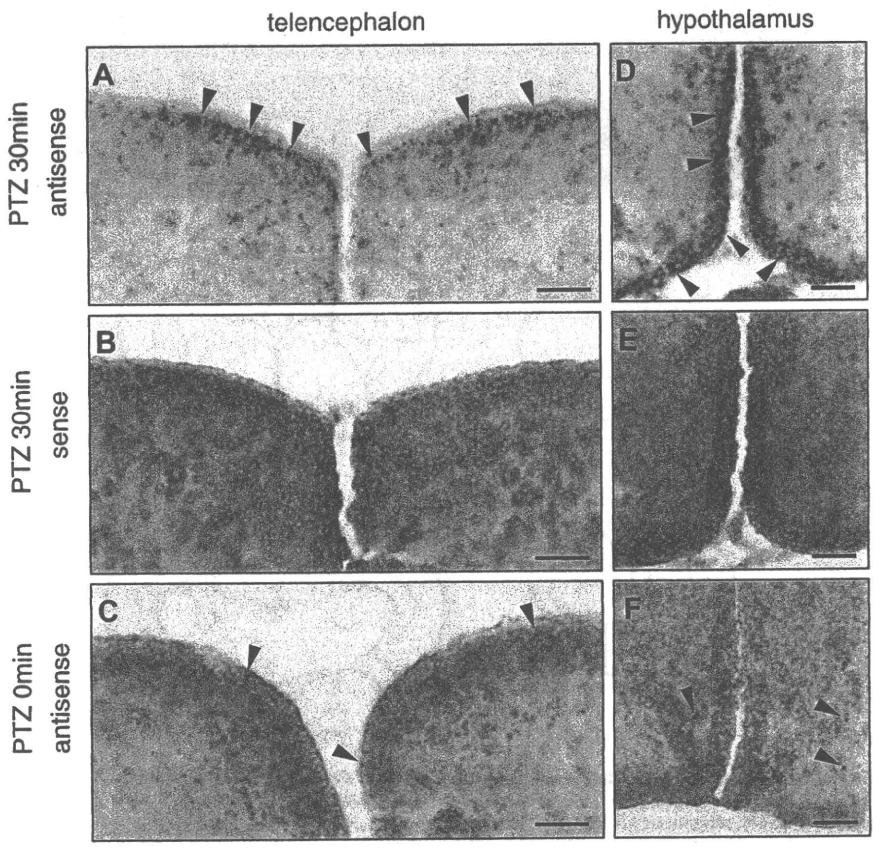

Fig. 3. Detection of the de novo synthesis of *c-fos* transcripts using *in situ* hybridization method. In the brains of medaka treated with 10-mM PTZ, dot-like signals were detected in the telencephalon (A; arrowhead) and hypothalamus (D; arrowhead). No significant signal was detected using the sense probe as a negative control (B and E) in cell nuclei. The number of dot-like signals increased depending on PTZ-treatment both in the telencephalon (C) and the hypothalamus (F). Scale bar, 50 mm.

Next, using this method, we compared the *c-fos* transcription before and after mating behavior in the female brain. We prepared a series of paraffin sections from the female brains 30 min after spawning and ejaculation. In the female brain, dot-like signals were detected in the preoptic area, optic tectum, and cerebellum (Fig. 4C–E). A large number of dot-like signals were detected in the dorsomedial telencephalon of females (Fig. 4B). The induction was not detected in the dorsolateral region of telencephalon (Supplementary Fig. S2B). The expression pattern was clearly different from that of PTZ-exposed medaka, where dot-like signals were detected in the dorsomedial and dorsolateral regions of telencephalon (Fig. 3A and Supplementary Fig. S2B). In contrast, a small number of dot-like signals were detected in the female brains before mating behavior (Fig. 4F–I and Supplementary Fig. S2B), and no dot-like signals were observed when the *c-fos* sense probe was used as a negative control (data not shown and Supplementary Fig. S2B).

4. Discussion

Here we identified a *c-fos* homologue gene in medaka and characterized the time course of its gene expression after pharmacologic stimulation. The *c-fos* expression peaked at 30-min post-induction and was markedly reduced at 90 min (Fig. 1A). The time course of *c-fos* mRNA induction was similar to that in mammals

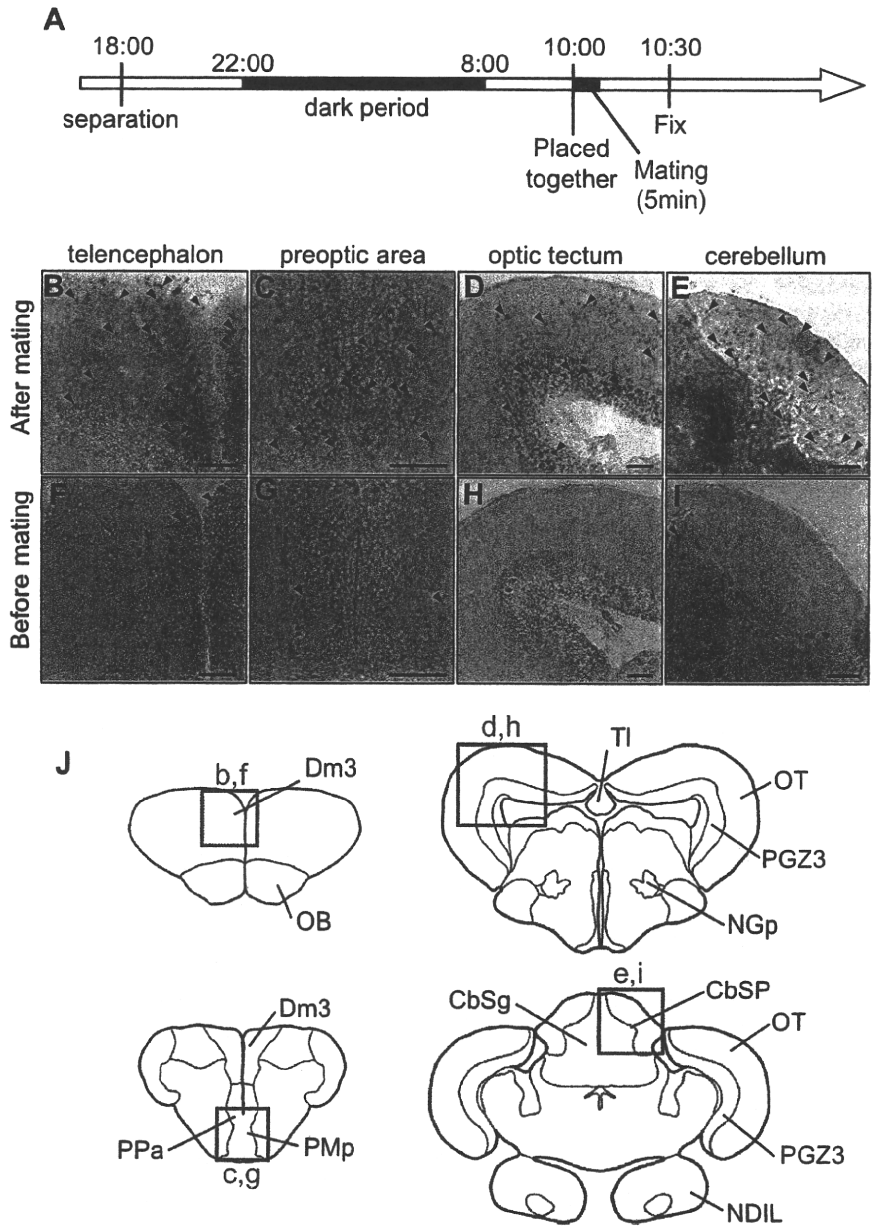

Fig. 4. Induction of the de novo synthesis of *c-fos* transcripts during mating. (A) Time course of the experiment. *c-fos* expression was detected by *in situ* hybridization using coronal brain sections after mating (B–E) and before mating (F–I). The dot-like signals (black arrowhead) were detected by *in situ* hybridization using coronal brain sections of female brain; medial telencephalon (B and F), preoptic area (C and G), optic tectum (D and H), and cerebellum (E and I). Scale bar, 50 mm. (J) Schematic presentation of the telencephalon, preoptic area, optic tectum and cerebellum of medaka brain. Areas corresponding to panels (B–I) are boxed in (J). The positions of the coronal sections are indicated in Supplementary Fig. S2. Dm3, area medialis3 of D; OB olfactory bulb; PPa, nucleus preopticus parvocellularis pars; PMp, nucleus preopticus magnocellularis pars parvocellularis; Tl torus longitudinalis; OT, tectum opticum; PGZ3 periventricular grey zone3; NGp nucleus glomerulosus posterioris; CbSg, stratum granulare of corpus cerebelli; CbSP, stratum Purkinje of corpus cerebelli; NDIL, nucleus diffuses of lobus inferioris.

[24]. A small increase in *c-fos* expression was also detected in control fish (Fig. 1A), which might be due to handling during transfer. Furthermore, qRT-PCR and *in situ* hybridization revealed that *c-fos* expression was induced in broad brain areas, including the telencephalon, optic tectum, and cerebellum in response to mating stimuli. In the present study, we performed *in situ* hybridization using a *c-fos* intron probe to detect only the immediate early induction of *c-fos* transcription (the de novo synthesis of *c-fos* transcripts). Generally, the use of intron-specific IEG riboprobes provides a marker of activated neuronal nuclei, without contamination by mature mRNA that can be encountered when using cDNA-based probes containing exonic sequences. Thus, use of the IEG intron probes can improve the temporal and spatial resolution of IEG mapping [23]. Furthermore, *in situ* hybridization signals using the IEG intron probes were detected in discrete intranuclear foci, which represented newly transcribed RNA at allelic sites [23]. In the present study, consistent with previous reports, the dot-like signals were detected using a *c-fos* intron probe.

The behavioral and pharmacologic induction of *c-fos* expression in medaka brain suggested that neural activity induces *c-fos* expression in medaka in a similar manner to that in mammals and birds. The merit of IEG mapping is that it allows us to simultaneously examine the response of multiple brain regions that are involved in natural behaviors under free-moving conditions. The present findings suggested widespread activation in the female brain following mating and we consider these results an initial step toward identifying the specific brain region involved in a behavioral element of female mating behavior, such as female choice and spawning. The medaka is a model organism for molecular biology and genetics [25] and efficient methods of generating both transgenic and knockout medaka are available [26,27]. Modulation of neural activity in target activated neurons using molecular techniques such as optogenesis [28] will lead to fine mapping of the neural circuit underlying mating behaviors.

Acknowledgments

We thank the Medaka National BioResource Project for providing the medaka strains. This work was supported by the Ministry of Education, Culture, Sports, Science, and Technology, Scientific Research on the Grant-in-Aid (Wakate B). The first author was supported by Grant-in-Aid for JSPS Fellows. This study was carried out under the NIBB Cooperative Research Program (10-104).

Appendix A. Supplementary data

Supplementary data associated with this article can be found, in the online version, at doi:10.1016/j.bbrc.2010.11.143.

References

[1] H. Imada, M. Hoki, Y. Suehiro, T. Okuyama, D. Kurabayashi, A. Shimada, K. Naruse, H. Takeda, T. Kubo, H. Takeuchi, Coordinated and cohesive movement of two small conspecific fish induced by eliciting a simultaneous optomotor response, PLoS ONE 5 (2010) e11248.
[2] K. Nakayama, Y. Oshima, K. Hiramatsu, Y. Shimasaki, T. Honjo, Effects of polychlorinated biphenyls on the schooling behavior of Japanese medaka (*Oryzias latipes*), Environ. Toxicol. Chem. 24 (2005) 2588–2593.
[3] J.J. Magnuson, An analysis of aggressive behaviour, growth, and competition for food and space in medaka (*Oryzias latipes*), Can. J. Zool. 40 (1962) 313–363.
[4] R.D. Howard, R.S. Martens, S.A. Innis, J.M. Drnevich, J. Hale, Mate choice and mate competition influence male body size in Japanese medaka, Anim. Behav. 55 (1998) 1151–1163.
[5] T. Ono, T. Uematsu, Mating ethogram in *Oryzias latipes*, J. Fac. Sci. Hokkaido. Univ. 13 (1957) 197–202.
[6] S. Fukamachi, M. Kinoshita, K. Aizawa, S. Oda, A. Meyer, H. Mitani, Dual control by a single gene of secondary sexual characters and mating preferences in medaka, BMC Biol. 7 (2009) 64.
[7] M. Furutani-Seiki, J. Wittbrodt, Medaka and zebrafish an evolutionary twin study, Mech. Dev. 121 (2004) 629–637.
[8] J.G. Pfaus, M.M. Heeb, Implications of immediate-early gene induction in the brain following sexual stimulation of female and male rodents, Brain Res. Bull. 44 (1997) 397–407.
[9] C.V. Mello, D.S. Vicario, D.F. Clayton, Song presentation induces gene expression in the songbird forebrain, Proc. Natl. Acad. Sci. USA 89 (1992) 6818–6822.
[10] K.L. Hoke, S.S. Burmeister, R.D. Fernald, A.S. Rand, M.J. Ryan, W. Wilczynski, Functional mapping of the auditory midbrain during mate call reception, J. Neurosci. 24 (2004) 11264–11272.
[11] L.M. Coolen, H.J.P.W. Peters, J.G. Veening, Fos immunoreactivity in the rat brain following consummatory elements of sexual behavior: a sex comparison, Brain Res. 738 (1996) 67–82.
[12] S.S. Burmeister, Genomic responses to behavioral interactions in an African cichlid fish: mechanisms and evolutionary implications, Brain Behav. Evol. 70 (2007) 247–256.
[13] S.S. Burmeister, R.D. Fernald, Evolutionary conservation of the egr-1 immediate-early gene response in a teleost, J. Comp. Neurol. 481 (2005) 220–232.
[14] S.S. Burmeister, E.D. Jarvis, R.D. Fernald, Rapid behavioral and genomic responses to social opportunity, PLoS Biol. 3 (2005) e363.
[15] Y. Suehiro, A. Yasuda, T. Okuyama, H. Imada, Y. Kuroyanagi, T. Kubo, H. Takeuchi, Mass spectrometric map of neuropeptide expression and analysis of the gamma-prepro-tachykinin gene expression in the medaka (*Oryzias latipes*) brain, Gen. Comp. Endocrinol. 161 (2009) 138–145.
[16] T. Kiya, T. Kunieda, T. Kubo, Increased neural activity of a mushroom body neuron subtype in the brains of forager honeybees, PLoS ONE 2 (2007) e371.
[17] M. Wada, N. Higo, S. Moizumi, S. Kitazawa, C-Fos expression during temporal order judgment in mice, PLoS ONE 5 (2010) e10483.
[18] S.C. Baraban, M.R. Taylor, P.A. Castro, H. Baier, Pentylenetetrazole induced changes in zebrafish behavior neural activity and c-FoS expression, Neuroscience 131 (2005) 759–768.
[19] J.I. Morgan, D.R. Cohen, J.L. Hempstead, T. Curran, Mapping patterns of c-fos expression in the central-nervous-system after seizure, Science 237 (1987) 192–197.
[20] M. Dragunow, H.A. Robertson, Generalized seizures induce c-fos protein(s) in mammalian neurons, Neurosci. Lett. 82 (1987) 157–161.
[21] P. Vanhoutte, J.V. Barnier, B. Guibert, C. Pages, M.J. Besson, R.A. Hipskind, J. Caboche, Glutamate induces phosphorylation of Elk-1 CREB, along with c-os activation, via an extracellular signal-regulated kinase-dependent pathway in brain slices, Mol. Cell. Biol. 19 (1999) 136–146.
[22] J. Hirayama, L. Cardone, M. Doi, P. Sassone-Corsi, Common pathways in circadian, cell cycle clocks light-dependent activation of Fos/AP-1 in zebrafish controls CRY-1a and WEE-1, Proc. Natl. Acad. Sci. USA 102 (2005) 10194–10199.
[23] J.F. Guzowski, J.A. Timlin, B. Roysam, B.L. McNaughton, P.F. Worley, C.A. Barnes, Mapping behaviorally relevant neural circuits with immediate-early gene expression, Curr. Opin. Neurobiol. 15 (2005) 599–606.
[24] W.E. Cullinan, J.P. Herman, D.F. Battaglia, H. Akil, S.J. Watson, Pattern and time course of immediate early gene expression in rat brain following acute stress, Neuroscience 64 (1995) 477–505.
[25] J. Wittbrodt, A. Shima, M. Schartl, Medaka – a model organism from the Far East, Nature Rev. Genet. 3 (2002) 53–64.
[26] Y. Taniguchi, S. Takeda, M. Furutani-Seiki, Y. Kamei, T. Todo, T. Sasado, T. Deguchi, H. Kondoh, J. Mudde, M. Yamazoe, M. Hidaka, H. Mitani, A. Toyoda, Y. Sakaki, R.H. Plasterk, E. Cuppen, Generation of medaka gene knockout models by target-selected mutagenesis, Genome Biol. 7 (2006) R116.
[27] S. Nakamura, D. Saito, M. Tanaka, Generation of transgenic medaka using modified bacterial artificial chromosome, Growth Differ. (2008) 415–419.
[28] H. Baier, E.K. Scott, Genetic and optical targeting of neural circuits and behavior – zebrafish in the spotlight, Curr. Opin. Neurobiol. 19 (2009) 553–560.

Tohoku J. Exp. Med., 2010, 221, 181-185

Liver Fibrosis in an Extremely Small Infant for Gestational Age

Hirokazu Arai,[1,2] Atsuko Noguchi,[1] Ryoji Goto,[2] Takefumi Matsuda,[2] Hatsushi Nakajima[2] and Tsutomu Takahashi[1]

[1]Department of Pediatrics, Akita University Graduate School of Medicine, Akita, Japan
[2]Department of Pediatrics, Akita Red Cross Hospital, Akita, Japan

Premature infants with intrauterine growth restriction (IUGR) are at greater risk for an adverse perinatal outcome. IUGR affects hepatocyte function, but the histopathological changes in the postnatal liver are not well known. We report a male infant with severe IUGR. His mother was transferred to our hospital at 26 weeks of gestation because of preterm labor and severe IUGR. An emergency cesarean section was carried out because of a non-reassuring fetal status. The birth weight of the infant was 332 g. He showed congestive heart failure and marked hepatomegaly from birth. After 1 week, blood examinations showed hyperbilirubinemia with high direct bilirubin. Because of liver dysfunction, he received the minimal total parenteral nutrition for 7 days. After 1 month, he progressively developed ascites and coagulopathy, and died 3 months after birth. Liver autopsy showed diffuse perisinusoidal fibrosis. Fibrosis was also prominent around the central vein. Immunohistochemical study revealed many α-smooth muscle actin-positive cells, which represent activated hepatic stellate cells, and a few transforming growth factor-β1-positive cells in the perisinusoidal fibrotic area. These results indicate that the infant developed chronic (end stage) liver failure by 3 months of age. We excluded congenital infection, metabolic syndrome and citrin deficiency. It is therefore conceivable that intrauterine cardiac failure may be responsible for liver fibrosis. Early detection of liver dysfunction soon after birth is a key to predict the prognosis of severe IUGR in preterm infants.

Keywords: liver failure; IUGR; preterm infant; liver fibrosis; extremely low birth weight
Tohoku J. Exp. Med., 2010, **221** (3), 181-185.

Premature infants with intrauterine growth restriction (IUGR) are at greater risk for postnatal growth and development as well as acute and chronic morbidities (Rosenberg 2008). IUGR influences hepatocyte function (Alonso et al. 2007). Compared to appropriate for gestational age (AGA) infants of similar birth weight, small for gestational age (SGA) infants show a higher rate of neonatal cholestasis (Boehm et al. 1990); however, only one report has shown postnatal liver histopathological changes for SGA infants that received prolonged total parenteral nutrition (TPN) (Baserga and Sola 2004).

Herein, we report the unusual case of an extremely low birth weight (ELBW) infant with severe IUGR. At birth, the infant showed congestive heart failure. Severe coagulopathy, thrombocytopenia, and jaundice persisted. The infant received the minimal TPN for only 7 days, and subsequently developed severe perisinusoidal liver fibrosis.

Patient Report

A 36-year-old woman, gravida 2, para 1, was referred to another hospital at 25 weeks of gestation with suspected IUGR. IUGR was first suspected at 23 weeks of gestation at another clinic. She was transferred to our hospital at 26 weeks of gestation because of preterm labor and severe IUGR. Ultrasound revealed severe growth restriction of the fetal biparietal diameter and abdominal circumference (each below -2 standard deviation). A first-trimester ultrasound had confirmed gestational age. She had reliable date parameters confirmed by the crown-rump length at 8 weeks' gestation. During her first pregnancy at 26 years old, she had undergone an artificial abortion. There had been no complications in her second pregnancy; a healthy child was born spontaneously at term. There was no family history of hereditary disorders. She had not taken medicine during the pregnancy. On admission, she did not have premature rupture of the membranes. Fetal ultrasound showed reverse end-diastolic flow in the umbilical artery and umbilical venous pulsations. Middle cerebral artery flow pattern showed redistribution (resistance index = 0.66). We did not examine the fetal karyotype because her family refused.

At 26 weeks of gestation, an emergency cesarean section was carried out because of a non-reassuring fetal status (minimal fetal heart rate variability). The birth weight of the male infant was 332 g. The infant had asphyxia, with Apgar scores of 3 at one minute and 5 at five minutes, and required resuscitation with tracheal intubation. On admis-

Received January 12, 2010; revision accepted for publication May 7, 2010. doi:10.1620/tjem.221.181
Correspondence: Hirokazu Arai, M.D., Ph.D., Department of Pediatrics, Akita University Graduate School of Medicine, Hondo 1-1-1, Akita, Akita 010-8543, Japan.
e-mail: arahiro@med.akita-u.ac.jp

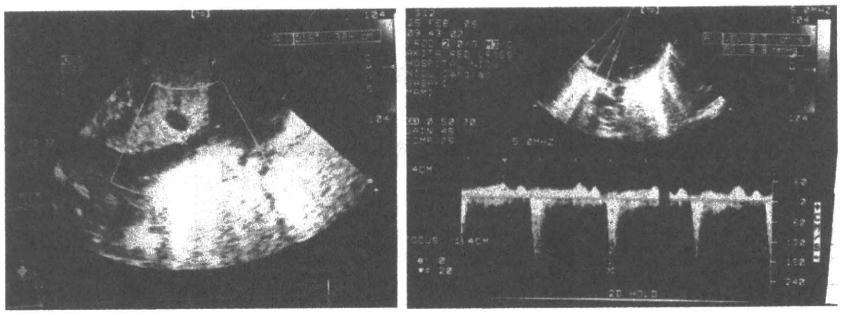

Fig. 1. Infant echocardiography. Echocardiography showed dilated inferior vena cava (left) and tricuspid regurgitation (right) at day 0.

Table1. Laboratory findings on admission (day 0).

pH	7.202	AST	52 U/L	Na	140 mmol/L
pCO2	35.7 mmHg	ALT	3 U/L	K	3.6 mmol/L
BE	−13.3 mEq/L	LDH	851 U/L	Cl	99 mmol/L
BS	127 mg/dL	GGT	204 U/L	Ca	9.4 mg/dL
		T.Bil	2.4 mg/dL	iP	5.2 mg/dL
WBC	3,600/μL	D.Bil	0.5 mg/dL	Fe	79 μg/dL
Hb	13.6 g/dL	ALP	199 U/L	IgG	353 mg/dL
Plt	$0.2 \times 10^4/\mu$L	CK	309 U/L	IgM	1 mg/dL
		TP	3.2 g/dL	CRP	0.0 mg/dL
APTT	69.9 sec	Alb	2.2 g/dL		
PT	34%	T.Chol	21 mg/dL		
Fib	< 50 mg/dL	TG	27 mg/dL		
D-dimer	2.0 mg/dL	BUN	9.7 mg/dL		
AT-III	< 20%	Cr	0.66 mg/dL		
HPT	24%				

sion, he had respiratory distress syndrome, and received artificial surfactant replacement therapy. A chest radiograph showed cardiomegaly. Echocardiography showed left ventricular dysfunction with ejection fraction of 46% (Murase et al. 2002), a dilated inferior vena cava, and tricuspid and mitral regurgitation (Fig. 1). Soon after birth, the patient showed congestive heart failure. Congenital cardiac malformation was absent. The patient was treated with inotropic and vasodilatory agents, and his cardiopulmonary condition improved gradually. No renal anomaly could be found on ultrasonography. Ophthalmological examination yielded normal findings. We could not examine his karyotype as the parents did not consent, but his face, appearance, and physical examination did not suggest trisomy 21 or 18.

Initial laboratory studies (Table 1) indicated a platelet count of $0.2 \times 10^4/\mu$L. Blood examinations showed metabolic acidosis (pH 7.202, BE -13.3 mmol/L), and coagulopathy was identified: fibrinogen (< 50 mg/dL) and prothrombin time (PT) % (34%) were low. Blood ammonia and blood glucose levels were within the normal ranges.

He showed marked hepatomegaly from birth. After 1 week, blood examinations showed hyperbilirubinemia with high direct bilirubin (total and direct bilirubin of 17.7 and 13.3 mg/dL at 17 days of life, respectively) (Fig. 2). Because of liver dysfunction, TPN (amino acids 0.3-1 g/kg/day; glucose infusion rate, max 6 mg/kg/minute; and vitamins) was used for only 7 days and we did not use intravenous lipid infusion; however, cholestasis did not improve, and we started ursodeoxycholic acid (UDC) (15 mg/kg/day).

After 1 month, he progressively presented with severe liver dysfunction with cholestasis, which led to the development of ascites, coagulopathy, and hypoalbuminemia. We administered fresh frozen plasma and vitamin K infusion frequently to improve coagulopathy, but these therapies were unsuccessful; his condition became unstable and he progressed to grade IV intraventricular hemorrhage. Plasma amino acid examination on day 91 showed hypertyrosinemia (1,113 nmol/mL). We suspected tyrosinemia type I, but no accumulation of upstream metabolites and succinylacetone was detected. Alpha-fetoprotein was 8,264.6 ng/mL (normal range) on the same day. Total bile acids were 119 μmol/L (day 91). We used special milk formulas (medium chain triglyceride (MCT)-enriched formulas or tyrosine-free milk), but his condition did not improve. He died 3 months after birth because of sepsis.

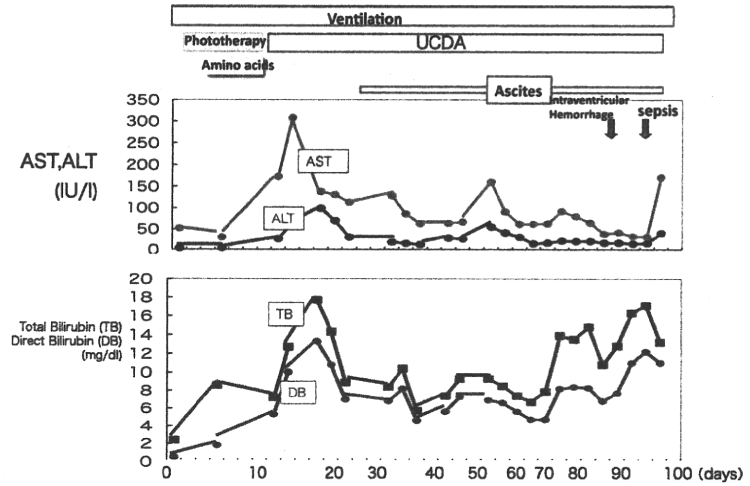

Fig. 2. Clinical course. After 1 week, blood examinations showed hyperbilirubinemia with high direct bilirubin.

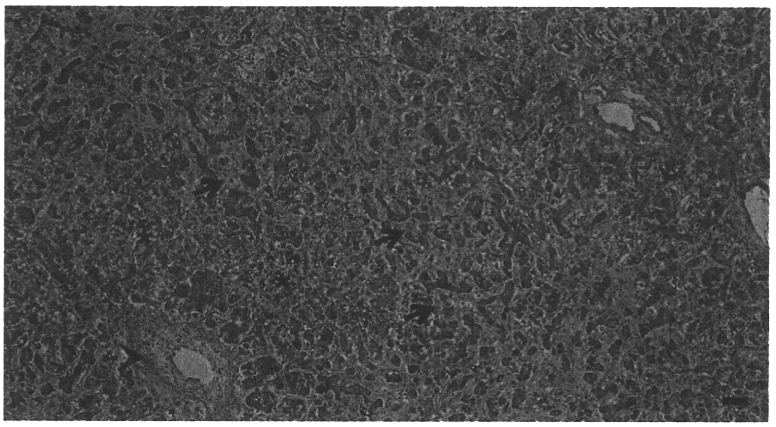

Fig. 3. Histology of the liver by Elastica-Masson staining. Liver specimens were fixed in formalin, embedded in paraffin, sectioned thinly, and stained with Elastica-Masson. Increased collagen fibers (arrows) were present along the sinusoids. Fibrosis was prominent around the central vein (arrowhead), and the hepatocytes showed frequent disruption (asterisk). Cellular infiltration of the parenchyma was absent. Fatty liver change was absent. Bar = 50 μm

After death, congenital infection (varicela zoster, herpes, cytomegalovirus, toxoplasmosis, syphilis, and rubella), extrahepatic obstruction, citrin deficiency (neonatal intrahepatic cholestasis), and inborn errors of bile acid metabolism (e.g., primary 3-oxo-delta 4-steroid 5 beta-reductase deficiency) were excluded. The results of neonatal screening for metabolic diseases (galactosemia, homocystiuria, phenylketouria, and maple syrup urine disease) and endocrine diseases (hypothyroidism and adrenal hyperplasia) were negative. A liver sample was the only specimen obtained after death with informed consent from the parents. No extrahepatic bilary atresia was noted. Microscopically, diffuse perisinusoidal liver fibrosis with increased collagen fibers was observed (Fig. 3). Fibrosis was prominent around the central vein, and the hepatocytes showed frequent disruption. Iron deposits were mildly present. Cellular infiltration in the parenchyma was absent. Fatty liver change was also absent (Fig. 3).

Immunohistochemically, many α-smooth muscle actin-positive cells, which represent activated hepatic stellate cells (HSCs), were detected in the perisinusoidal fibrotic area (Fig. 4a and c); moreover, a few transforming growth factor (TGF)-β1-positive cells were present in the same area (Fig. 4b and d).

Discussion

This patient received TPN for only 1 week because of cholestasis. In spite of minimal TPN, he showed severe liver fibrosis. Baserga et al. (2004) reported that SGA-ELBW infants have a risk factor for TPN (for >7 days)-associated cholestasis. Some of these infants showed portal/sinusoidal fibrosis; however, compared with our patient, they used higher doses of amino acids, glucose and intravenous lipids.

Moreover, infection, metabolic disease, and heart failure contribute to liver failure (cholestasis in neonates and infants) (Alonso et al. 2007); however, we excluded con-

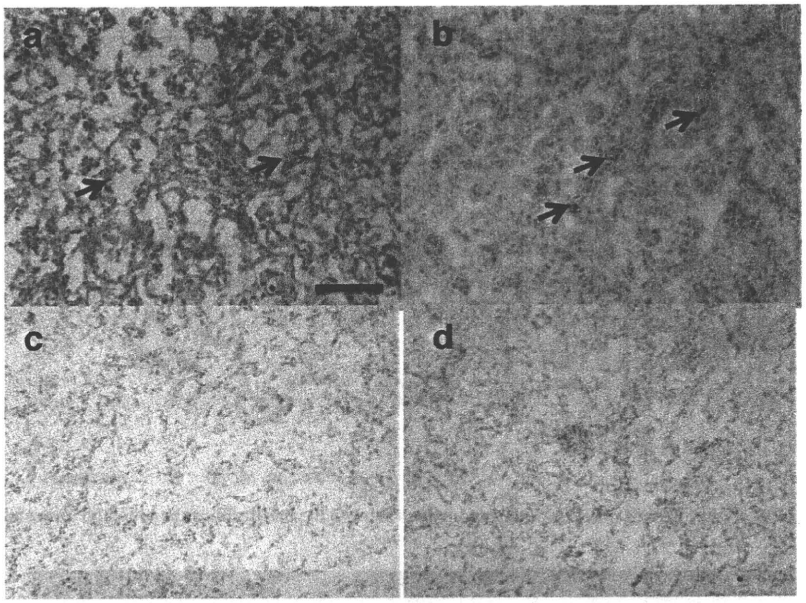

Fig. 4. Immunohistochemical staining of the liver. Immunohistochemical staining was performed using frozen sections. Antibodies against α-smooth muscle actin (a) (Boehringer Mannheim, Mannheim, Germany, dilution: 1:10) and TGF-β1 (b) (Santa Cruz Biotechnology, Inc., CA, USA, dilution: 1:200) were obtained commercially. (a) Immunoreactivity of spindle-like cells (arrows) was found along sinusoids. (b) Immunoreactivity was detected in round cells (arrows) in sinusoidal areas. (c) Negative control section for (a). (d) Negative control section for (b). Bar = 50 μm

genital infection, metabolic syndrome, and neonatal intrahepatic cholestasis.

Our patient showed hypertyrosinemia, but we excluded tyrosinemia type I because of no accumulation of upstream metabolites and succinylacetone. SGA infants are more sensitive to metabolic imbalances than AGA infants (Baserga et al. 2004). Also, Robles et al. (1984) reported hypertyrosinemia in small-for-date (SFD) infants. Hypertyrosinemia results from immature function of the enzyme 4-hydroxyphenylpyruvate dioxygenase, most frequently in premature infants (Russo et al. 2001).

A cause of IUGR is uteroplacental insufficiency secondary to maternal morbidities such as hypertension (Baserga et al. 2004). IUGR fetuses demonstrate progressive hemodynamic changes, and develop earlier and more pronounced right than left ventricular function deterioration (Bahtiyar and Copel 2008). Soon after birth, this patient showed congestive heart failure, which is associated with the development of liver fibrosis (Naschitz et al. 2000). An animal-based study of right ventricular pressure overload showed liver fibrosis and α-smooth muscle actin expression (Gieling et al. 2004). Although it could not be excluded that liver failure had been caused by another etiology, we suggested that intrauterine cardiac failure contributed to liver fibrosis.

An immunohistochemical study showed many α-smooth muscle actin-positive cells (myofibroblasts) and a few TGF-β1-positive cells in the perisinusoidal fibrotic area. Liver fibrosis contributes to the differentiation of HSCs into myofibroblasts (Hinz et al. 2007). TGF-β1 is the most potent profibrogenic cytokine that activates HSC, but the present patient showed only a few TGF-β1-positive cells, despite that fibrotic changes developed in the liver at 3 months of age.

Early detection of liver dysfunction (including the examination of markers of liver fibrosis) soon after birth is a key to predict the prognosis of severe IUGR in preterm infants.

References

Alonso, E.A., Squires, R.H. & Whitington, P.F. (2007) Acute liver failure in children. In *Liver disease in children*, edited by F.J. Suchy. Cambridge University Press, NY, pp. 71-96.

Bahtiyar, M.O. & Copel, J.A. (2008) Cardiac changes in the intrauterine growth-restricted fetus. *Semin. Perinatol.*, **32**, 190-193.

Baserga, M.C. & Sola, A. (2004) Intrauterine growth restriction impacts tolerance to total parenteral nutrition in extremely low birth weight infants. *J. Perinatol.*, **24**, 476-481.

Boehm, G., Müller, D.M., Teichmann, B. & Krumbiegel, P. (1990) Influence of intrauterine growth retardation on parameters of liver function in low birth weight infants. *Eur. J. Pediatr.*, **149**, 396-398.

Gieling, R.G., Ruijter, J.M., Maas, A.A., Van Den Bergh Weerman, M.A., Dingemans, K.P., ten Kate, F.J., Lekanne dit Deprez, R.H., Moorman, A.F. & Lamers, W.H. (2004) Hepatic response to right ventricular pressure overload. *Gastroenterology*, **127**, 1210-1221.

Hinz, B., Phan, S.H., Thannickal, V.J., Galli, A., Bochaton-Piallat, M.L. & Gabbiani, G. (2007) The myofibroblast: one function, multiple origins. *Am. J. Pathol.*, **170**, 1807-1816.

Murase, M., Ishida, A. & Momota, T. (2002) Serial pulsed Doppler assessment of early left ventricular output in critically ill very low-birth-weight infants. *Pediatr. Cardiol.*, **23**, 442-448.

Naschitz, J.E., Slobodin, G., Lewis, R.J., Zuckerman, E. & Yeshurun, D. (2000) Heart diseases affecting the liver and liver diseases affecting the heart. *Am. Heart J.*, **140**, 111-120.

Robles, R., Gil, A., Faus, M.J., Periago, J.L., Sánchez-Pozo, A., Pita, M.L. & Sánchez-Medina, F. (1984) Serum and urine amino acid patterns during the first month of life in small-for-date infants. *Biol. Neonate*, **45**, 209-217.

Rosenberg, A. (2008) The IUGR newborn. *Semin. Perinatol.*, **32**, 219-224.

Russo, P.A., Mitchell, G.A. & Tanguay, R.M. (2001) Tyrosinemia: a review. *Pediatr. Dev. Pathol.*, **4**, 212-221.

J Inherit Metab Dis
DOI 10.1007/s10545-010-9168-5

RESEARCH REPORT

A neonatal-onset succinyl-CoA:3-ketoacid CoA transferase (SCOT)-deficient patient with T435N and c.658-666dupAACGTGATT p.N220_I222dup mutations in the *OXCT1* gene

Toshiyuki Fukao · Tomohiro Ishii · Naoko Amano · Petri Kursula · Masaki Takayanagi · Keiko Murase · Naomi Sakaguchi · Naomi Kondo · Tomonobu Hasegawa

Received: 30 March 2010 / Revised: 30 June 2010 / Accepted: 2 July 2010

Abstract Succinyl-CoA:3-ketoacid CoA transferase (SCOT) deficiency causes episodic ketoacidotic crises and no apparent symptoms between them. Here, we report a Japanese case of neonatal-onset SCOT deficiency. The male patient presented a severe ketoacidotic crisis, with blood pH of 7.072 and bicarbonate of 5.8 mmol/L at the age of 2 days and was successfully treated with intravenous infusion of glucose and sodium bicarbonate. He was diagnosed as SCOT deficient by enzymatic assay and mutation analysis. At the age of 7 months, he developed a second ketoacidotic crisis, with blood pH of 7.059, bicarbonate of 5.4 mmol/L, and total ketone bodies of 29.1 mmol/L. He experienced two milder ketoacidotic crises at the ages of 1 year and 7 months and 3 years and 7 months. His urinary ketone bodies usually range from negative to 1+ but sometimes show 3+ (ketostix) without any symptoms. Hence, this patient does not show permanent ketonuria, which is characteristic of typical SCOT-deficient patients. He is a compound heterozygote of c.1304C > A (T435N) and c.658-666dupAACGTGATT p.N220_I222dup. mutations in the *OXCT1* gene. The T435N mutation was previously reported as one which retained significant residual activity. The latter novel mutation was revealed to retain no residual activity by

Communicated by: K. Michael Gibson

References to electronic databases: Succinyl-CoA:3-ketoacid CoA transferase deficiency (OMIM 245050 601424): Succinyl-CoA:3-ketoacid CoA transferase (EC 2.8.3.5): *OXCT1* gene (gene ID 5019 NM_000436)

Competing interests: None declared.

T. Fukao · K. Murase · N. Sakaguchi · N. Kondo
Department of Pediatrics, Graduate School of Medicine,
Gifu University,
1-1 Yanagido,
Gifu, Gifu 501-1194, Japan

T. Fukao (✉)
Medical Information Sciences Division,
United Graduate School of Drug Discovery and Medical Information Sciences, Gifu University,
1-1 Yanagido,
Gifu, Gifu 501-1194, Japan
e-mail: toshi-gif@umin.net

T. Fukao
Clinical Research Division, Nagara Medical Center,
Gifu, Gifu 502-8558, Japan

T. Ishii · N. Amano · T. Hasegawa
Department of Pediatrics, Keio University School of Medicine,
Shinjuku, Tokyo 160-8582, Japan

P. Kursula
Department of Biochemistry, University of Oulu,
P.O. Box 3000, FIN-90014 Oulu, Finland

M. Takayanagi
Chiba Children's Hospital,
Chiba, Chiba 266-0007, Japan

Published online: 21 July 2010

transient expression analysis. Both T435N and N220_I222 lie close to the SCOT dimerization interface and are not directly connected to the active site in the tertiary structure of a human SCOT dimer. In transient expression analysis, no apparent interallelic complementation or dominant negative effects were observed. Significant residual activity from the T435N mutant allele may prevent the patient from developing permanent ketonuria.

Abbreviations

SCOT succinyl-CoA:3-ketoacid CoA transferase
TKB total ketone bodies
FFA free fatty acids

Introduction

Ketone bodies, produced mainly in the liver, are an important source of energy for extrahepatic tissues (Mitchell and Fukao 2001). Succinyl-CoA: 3-ketoacid CoA transferase (SCOT; EC 2.8.3.5) is a mitochondrial homodimer essential for ketone body utilization. SCOT deficiency (OMIM 245050) causes episodic ketoacidosis and is part of the differential diagnosis of childhood ketoacidosis, a frequently occurring condition. In contrast with most organic acidemias, no diagnostic metabolites are observed in the blood and urine samples from SCOT-deficient patients, although the ketone bodies, acetoacetate, and 3-hydroxybutyrate are elevated (Mitchell and Fukao 2001). Since the first description of SCOT deficiency (Cornblath et al. 1971; Tildon and Cornblath 1972), fewer than 30 affected probands have been reported, including personal communication (Saudubray et al. 1987; Perez-Cerda et al. 1992; Sakazaki et al. 1995; Fukao et al. 1996, 2000, 2004, 2006; Pretorius et al. 1996; Niezen-Koning et al. 1997; Rolland et al. 1998; Snyderman et al. 1998; Berry et al. 2001; Longo et al. 2004; Yamada et al. 2007; Merron and Akhtar 2009; and seven other unpublished cases sent to TF). Because of the nonspecific metabolite profile of SCOT-deficient patients, in vitro methods of diagnosis are particularly important. Enzyme assays of SCOT activity are sufficient for clinical diagnosis, but current whole-cell assays can yield a spuriously high apparent residual activity (Perez-Cerda et al. 1992; Sakazaki et al. 1995; Kassovska-Bratinova et al. 1996). To assist clinical diagnosis, we cloned the human SCOT complementary DNA (cDNA) (Kassovska-Bratinova et al. 1996) and SCOT gene (*OXCT1*, Fukao et al. 2000), developed an anti-(human SCOT) antibody (Song et al. 1997), and described ten *OXCT1* gene mutations in SCOT-deficient patients (Kassovska-Bratinova et al. 1996; Song et al. 1998; Fukao et al. 2000, 2004, 2006, 2007; Longo et al. 2004; Yamada et al. 2007).

SCOT deficiency is one of the most important differential diagnosis of neonatal ketoacidotic crisis, since about half of the reported SCOT-deficient patients developed their first ketoacidotic crises in the neonatal period (Mitchell and Fukao 2001). Persistent ketosis and ketonuria are pathognomonic features of SCOT deficiency; however, these are not present in all SCOT-deficient patients. We previously pointed out that patients with mutation T435N, which retained some residual SCOT activity, do not show permanent ketosis (Fukao et al. 2004). In this study, we describe a Japanese SCOT-deficient patient with neonatal onset. One of his mutations was revealed to be T435N.

Materials and methods

Case presentation

The proband (GS21) is a Japanese boy born from non-consanguineous parents at 38 weeks of gestation. The pregnancy and delivery were uneventful. His birth length was 49.1 cm (50th–90th percentile), weight 2.59 kg (3rd–10th percentile), and head circumference 34.3 cm (50th–90th percentile). At the age of 2 days, he presented tachypnea and poor drinking ability. Physical examination revealed grunting and sternal retraction with a respiration rate of 60/min. Blood gas analysis showed severe metabolic acidosis [pH 7.072, partial pressure of carbon dioxide (PCO_2) 20.5 mmHg, bicarbonate 5.8 mmol/L]. The blood glucose level was 3 mmol/L, ammonia 95 μmol/L, sodium (Na) 151 mEq/L, potassium (K) 4.19 mEq/L, chlorine (Cl) 113.1 mEq/L, and urinary ketone bodies 3+ (ketostix, Siemens Healthcare Diagnostics, USA). GS21 was treated by intravenous infusion of glucose and sodium bicarbonate. Urinary organic-acid analysis by gas chromatography-mass spectrometry showed massive amounts of 3-hydroxybutyrate and acetoacetate with dicarboxylic acids. He was transferred to Keio University Hospital for further evaluation at 4 days of age. On admission, his general condition and blood gas data (pH 7.453, PCO_2 24.4 mmHg, bicarbonate 20.4 mmol/L) improved with intravenous infusion of glucose at 7 mg/kg/min. GS21 was suspected of having SCOT deficiency, and this was confirmed by enzyme assay using peripheral blood mononuclear cells and mutation analysis (see "Results and Discussion"). At the age of 3 weeks, serum free fatty acids (FFA) and total ketone bodies (TKB) were measured at 1, 3, and 6 h after feeding, as shown in Table 1. At the age of 1 month, the boy was discharged from the hospital. The feeding interval was kept at <6 h to avoid severe ketoacidosis.

At the ages of 3 months and 4 months, FFA and TKB (3 h after feeding) were measured, as shown in Table 1. TKB levels became higher than those at the age of 3 weeks.

Table 1 Serum free fatty acids (FFA) and total keytone bodies (TKB)

Age		FFA (mM)	TKB (mM)	FFA/TKB
3 weeks	1 h after feeding	0.20	0.24	0.83
	3 h after feeding	0.17	0.15	1.13
	6 h after feeding	0.46	0.81	0.57
3 months	3 h after feeding	0.53	2.54	0.21
4 months	3 h after feeding	0.39	1.49	0.26
7 months	Ketoacidotic crisis	1.84	29.1	0.06
	2 days after crisis	0.97	0.54	1.80
1.5 years	Mild ketoacidotic crisis	ND	10.3	NA
3 years 7 months	Mild ketoacidotic crisis	1.61	11.2	0.14
Reference values*	Fed state		0.10-0.30	
	15-h fast	0.5-1.6	0.10-0.70	0.6-5.2

ND not determined, *NA* not applicable

*Reference values are from Bonnefont et al. 1990

At the age of 7 months, he developed his second ketoacidotic crisis for no clear reason and was again hospitalized. The laboratory findings were blood pH 7.059, PCO_2 20.2 mmHg, bicarbonate 5.4 mmol/L, glucose 2.2 mmol/L, and TKB 29.1 mmol/L. Treatment was begun with intravenous infusion of glucose at 5.5–7.1 mg/kg/min. He had a bolus injection of 1 mEq/kg of sodium bicarbonate followed by continuous infusion of sodium bicarbonate at 1 mEq/kg/h for 8 h. Thirteen hours after admission, continuous infusion of insulin was also initiated at a glucose/insulin ratio of 6.2–8.3 g/U, since his blood glucose levels were rather high (11.0 mmol/L). The urinary ketone bodies turned negative 2 days after admission. At the ages of 1 year 7 months and 3 years 7 months, he exhibited his third and fourth episodes of ketoacidotic crisis due to acute gastroenteritis. Blood pH was 7.280, PCO_2 20.3 mmHg, bicarbonate 9.2 mmol/L, and TKB 10.3 mmol/L in the third episode, and blood pH was 7.192, PCO_2 17.3 mmHg, bicarbonate 6.4 mmol/L in the fourth episode. FFA and TKB during the episodes are shown in Table 1. GS21 recovered by continuous infusion of glucose only during both episodes. At the age of 3 years and 5 months, he was 93.4 cm in height (50th percentile), 11.95 kg in weight (10th percentile), and had a head circumference of 50.4 cm (50th–75th percentile). The patient is now 3 years and 9 months old, and his motor and mental development are within normal range. The feeding interval has been prolonged up to 12 h. His urinary ketone bodies usually range from negative to 1+ but sometimes show 3+ without any symptoms.

Enzyme assay

Informed consent for enzymatic diagnosis and molecular analysis was obtained from the parents of GS21. This study was approved by the Ethical Committee of the Graduate School of Medicine, Gifu University. Assays for acetoacetyl-CoA thiolase and for SCOT were as previously described (Fukao et al. 1997; Song et al. 1997) using acetoacetyl-CoA as a substrate and measuring its disappearance spectrophotometrically.

Mutation analysis

Total RNA was purified from peripheral blood mononuclear cells with an ISOGEN kit (Nippon Gene, Tokyo, Japan). Real-time polymerase chain reaction (RT-PCR) was as previously described (Kassovska-Bratinova et al. 1996). Mutations were detected by amplifying cDNA spanning the full-length coding sequence and by sequencing ten clones. Genomic DNA was purified with a Sepa Gene kit (Sanko Junyaku, Tokyo, Japan). Mutation analysis at the genomic level was done by PCR for each exon and its intron boundaries (at least 50 bases from the exon/intron boundaries for both directions), followed by direct sequencing (Fukao et al. 2000).

Transient expression analysis

Mutant expression vectors were made using a QuikChange Site-Directed Mutagenesis kit (Stratagene, La Jolla, CA, USA) and were confirmed by sequencing. Wild-type and mutant SCOT expression vectors (4 μg) were first transfected using Lipofectamine 2000 (GIBCO BRL Invitrogen Inc., Carlsbad, CA, USA) in ~10^5 SV40-transformed SCOT-deficient fibroblasts of GS01 (Kassovska-Bratinova et al. 1996; Fukao et al. 2004). One microgram of the cytosolic acetoacetyl-CoA thiolase (CT)-expressing vector, pCAGGSct (Song et al. 1994), was cotransfected to monitor transfection efficiency. Transfection was done at 37°C for 24 h, then a further 48-h incubation was done at 37°C. The cells were harvested and stored at –80°C until SCOT and CT activities were assayed. Immunoblotting was done using a mixture of an anti-(human SCOT) antibody

(Song et al. 1997) and anti-(human CT) antibody (Song et al. 1994) as the first antibody (Fukao et al. 1997). The quantity of the mutant protein was estimated densitometrically, comparing it to the signal intensities of serially diluted samples of the wild-type SCOT protein.

Structural analysis

For analyzing putative structural effects of mutations on the SCOT protein, the recently determined crystal structure from the Structural Genomics Consortium [Protein Data Bank (PDB) entry 3DLX] of human SCOT was taken as a starting point. The structure was subjected to further crystallographic refinement using PHENIX (Adams et al. 2010) and COOT (Emsley and Cowtan 2004), including the addition of missing side chains and rebuilding the solvent network.

Results and discussion

Molecular diagnosis and characterization of mutations

SCOT activity in GS21's peripheral blood mononuclear cells was apparently much lower than two controls (GS21:0.25, control 1: 2.4, control 2: 3.9 nmol/min/mg of protein). Hence, we tentatively diagnosed him as having SCOT deficiency. Since we could not draw blood for a repeat of the enzyme assay at the age of 1 month and skin biopsy was not acceptable to the parents, we performed mutation analysis to confirm the diagnosis. The full coding sequence of SCOT cDNA from GS21 was sequenced after subcloning. Mutations c.658-666dupAACGTGATT p.N220_I222dup. and c.1304C > A (T435N) were separately identified in six and four clones, respectively. No other mutations were found at the cDNA level. We

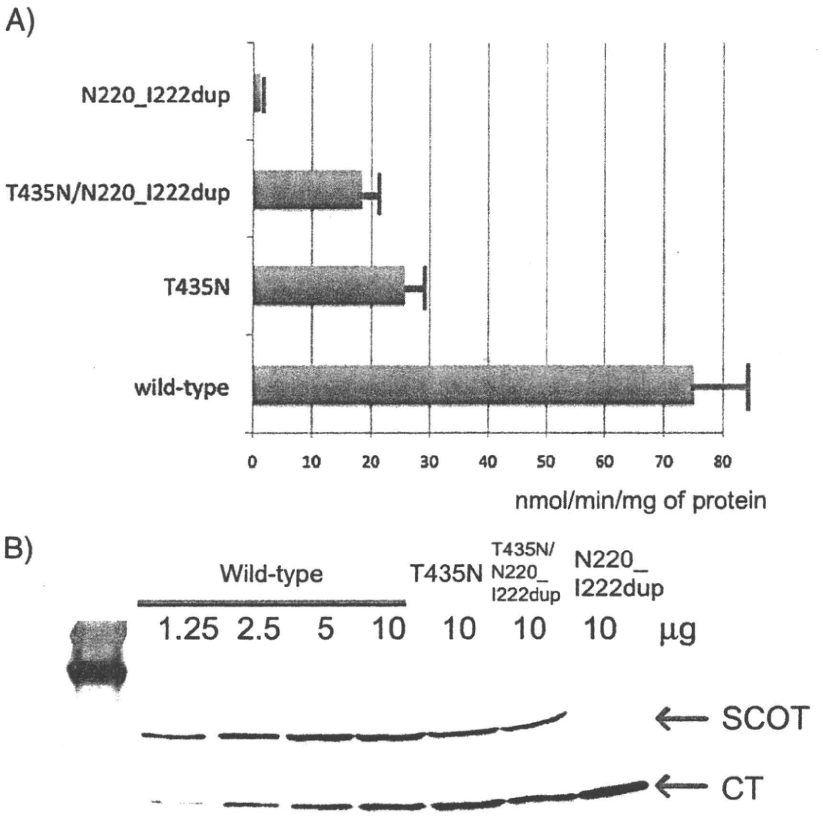

Fig. 1 Transient expression analysis of T435N and N220_I222dup mutant complementary DNAs (cDNAs). Transient expression analysis was performed at 37°C. Expression vectors (4 µg) were transfected. *T435N/ N220_I222dup* indicates a cotransfection of 4 µg each of two mutant expression vectors for T435N and N220_I222dup. **a** Succinyl-CoA:3-ketoacid CoA transferase (SCOT) enzyme assay. SCOT activity in the supernatant of the cell extract was measured. The mean values are shown together with the standard deviation (SD) of three independent experiments. **b** Immunoblot analysis. The protein amounts applied are shown *above the lanes*. We used previously described rabbit polyclonal antibodies, which we made (Song et al. 1994, 1997), and ProtoBlot Western blot AP system (Promega, Madison, WI, USA). The first antibody was a mixture of an anti-human cytosolic thiolase (CT) antibody and anti-human SCOT antibody. The positions of the bands for CT and SCOT are indicated by *arrows*. Immunoblotting was done using a mixture of an anti-(human SCOT) antibody (Song et al. 1997) and anti-(human CT) antibody (Song et al. 1994) as the first antibody (Fukao et al. 1997)

confirmed these mutations at the genomic level. Familial analysis showed that the 9-bp duplication was inherited from the mother and c.1304C > A (T435N) from the father. The 9-bp duplication was a novel mutation and T435N was previously reported in Japanese patients (Fukao et al. 2004).

Transient expression analysis of the c.658-666dupAACGT GATT p.N220_I222dup cDNA showed no residual activity (Fig. 1a), and the N220_I222dup SCOT protein was not detected in immunoblot analysis (Fig. 1b). Since SCOT protein is a homodimer and the T435N mutant retains significant residual SCOT activity, as previously reported (Fukao et al. 2004), we investigated possible interallelic influence between T435N and N220_I222dup by cotransfection of these two mutant cDNAs. However, no apparent interallelic complementation or dominant negative effect were observed.

The T435N mutation was previously identified in two Japanese SCOT-deficient families from the Amami islands (Fukao et al. 2004). There was no apparent consanguinity or relationship between these two families, and the patients were homozygotes of T435N. Since the Amami islands have a population of about 120,000, this mutation might be prevalent in that region. However, the father of GS21, who carries the T435N mutation, has no relation to the islands as far as he knows.

Recently, the crystal structure of human SCOT was determined (PDB entry 3DLX). The SCOT protein is a homodimer; both T435 and N220_I222 lie close to the SCOT dimerization interface and are not directly connected to the active site. Their overall localization in the context of the dimer is shown in Fig. 2a. T435 lies in a loop, with the side chain pointing inward to a rather hydrophilic environment (Fig. 2b); the hydroxyl group makes a hydrogen bond with a backbone carbonyl group from V394. Thus, it is expected that a T435N substitution will perturb the SCOT structure only a little, being able to make hydrogen bond interactions. This is also reflected in the fact that the T435N mutation is associated with significant residual SCOT activity. NVI220-222 is a short beta strand from a beta sandwich domain involved in SCOT dimerization (Fig. 2c). This small domain also contains other previously identified SCOT point mutations, namely, G219E, V221M, R224K, and R268H (Fukao et al. 2000, 2007; Yamada et al. 2007), making it a hot-spot for SCOT mutations. The small beta sandwich is tightly folded, and

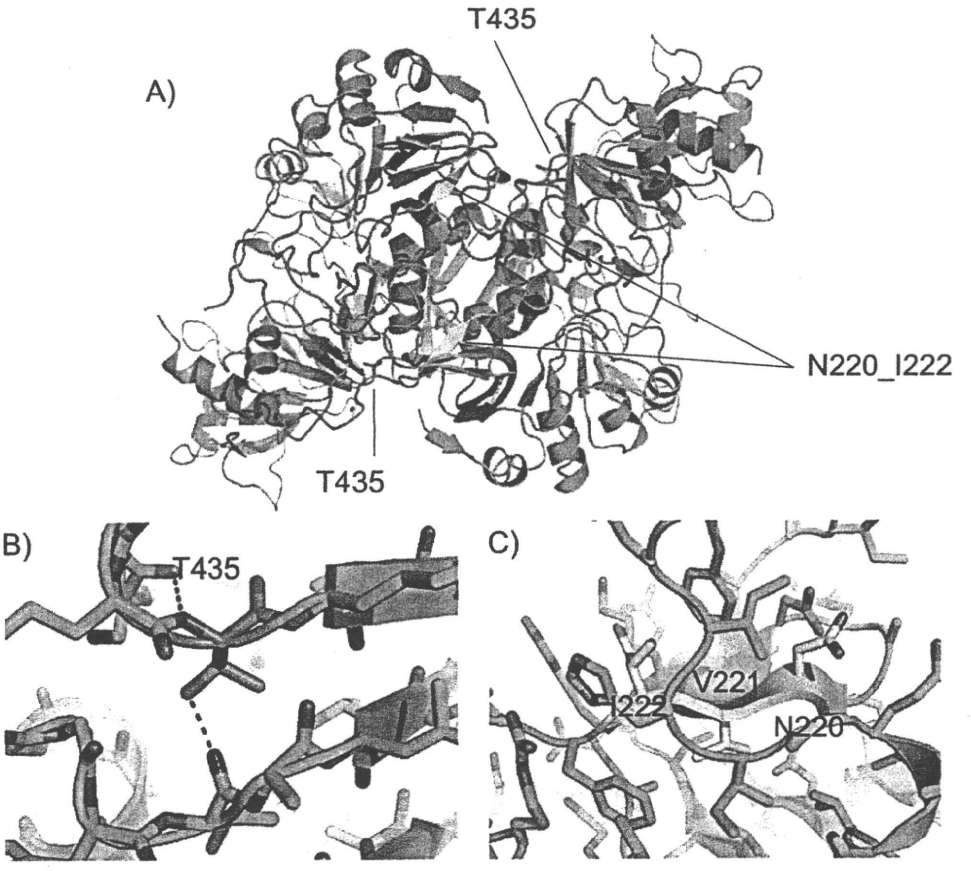

Fig. 2 Tertiary structure around mutations. **a** A human succinyl-CoA:3-ketoacid CoA transferase (SCOT) dimer, with E344 (highlighting the active site of SCOT) in *blue*, N220_I222 in *yellow*, and T435 in *orange*. The two monomers are shown in *green and light blue*. **b** Detailed surroundings of T435 (*orange*). Note the side chain is buried in a hydrophilic environment, making a hydrogen bond with a backbone oxygen. There are also additional potential hydrogen bonding partners in the vicinity. **c** The N220_I222 (in *yellow*) correspond to a short buried beta strand in a tightly packed environment. The dimer interface is at the *top* in this view

one can expect a duplication of three residues within the beta strand to disrupt its folding. This might affect the overall folding of the SCOT monomer and/or the formation of functional SCOT dimers.

Clinical issues

GS21 developed his first ketoacidotic crisis at the age of 2 days, although one of his mutated alleles retained residual SCOT activity. Almost half of the patients with SCOT deficiency develop their first ketoacidotic crisis at the age of 2–4 days (Mitchell and Fukao 2001). We summarized the mutations and their clinical phenotypes for several SCOT-deficient patients, including GS21, in Table 2. GS10, a homozygote of the R268H mutation, which retained residual activity, also developed his first ketoacidotic crisis at the age of 2 days, whereas his sibling (GS10s) with the same mutation developed her first crisis at the age of 6 months (Fukao et al. 2007). On the other hand, GK15, a homozygote of the null mutation, R217X, developed her first ketoacidotic crisis at the age of 8 months (Longo et al. 2004). Neonatal onset, hence, does not appear to be related to residual SCOT activity.

Permanent ketosis, or ketonuria, is a pathognomonic feature of SCOT deficiency (Mitchell and Fukao 2001). We previously reported that patients (GS08, GS09, and GS09b) who are homozygous for T435N did not show permanent ketosis or ketonuria (Fukao et al. 2004). In the case of GS21, the blood levels of FFA and TKB at 3 h after feeding were measured at the ages of 3 weeks, 3 monthsm and 4 months (Table 1). The level of TKB at the age of 3 weeks (0.15 mmol/L) was much less than those at the ages of 3 months and 4 months (2.54, 1.59 mmol/L, respectively). The FFA/TKB ratio at the ages of 3 and 4 months was 0.21 and 0.26, respectively, but was nearly 1.0 at the age of 3 weeks. In the cases of SCOT-deficient patients, this ratio was reported to be <0.3 early in a fasting test (Bonnefont et al. 1990). Even at 6 h after feeding at the age of 3 weeks, the level of TKB was 0.81 and the ratio was 0.57. These facts may mean that a hyperketotic status is not apparent during a nonepisodic condition in the neonatal period. The blood levels of FFA and TKB were not available during the age of 2–3 years, but urinary ketone bodies varied from negative to 3+ without any symptoms in GS21 and were always positive in GS02 and GS02s, whose mutations do not retain residual SCOT activity (Sakazaki et al. 1995). Hence, GS21 has no permanent ketonuria. It is very important to state that SCOT deficiency is the most probable diagnosis if permanent ketosis/ketonuria is present but that SCOT deficiency is not excluded even if permanent ketosis/ketonuria is absent.

Table 2 Succinyl-CoA:3-ketoacid CoA transferase (SCOT)-deficient patients

Number	Country	Sex	Mutations	Res. activity[a]	Onset	First ketoacidotic crisis				PK[b]	No. of episodes	Prognosis	References	
						pH	HCO3	TKB	glucose					
GS02	Japan	M	V133E/C456F	–	6mo	7.08	5.1	12.2	6.7	+	3	Good	Sakazaki et al. 1995	Song et al. 1998
GS02s	Japan	F	V133E/C456F	–	prenatal diagn.					+	1	Good	Fukao et al. 1996	Song et al. 1998
GS10	South Africa	M	R268H/R268H	+	2d	6.94	5	14.2	4.4	–	>5	Good	Pretorius et al. 1996	Fukao et al. 2007
GS10s	South Africa	F	R268H/R268H	+	6mo	7.12	8	5.1	6.6	–	5	Good	Pretorius et al. 1996	Fukao et al. 2007
GS15	USA	F	R217X/R217X	–	8mo	6.98	<5			+	1	Good	Longo et al. 2004	
GS08	Japan	M	T435N/T435N	+	1y5m	7.12	3.7	18.5	6.0	–	3	Good	Fukao et al. 2004	
GS09	Japan	M	T435N/T435N	+	10mo	7.00	5.8			–	>5	Good	Fukao et al. 2004	
GS09b	Japan	M	T435N/T435N	+	10mo	7.09	5.4		7.1	–	4	Good	Fukao et al. 2004	
GS21	Japan	M	T435N/N220_I222dup	+	2d	7.02	5.8		3	–	3	Good	This study	

[a] Residual SCOT activity in transient expression analysis of mutant complementary DNAs, [b] permanent ketosis

Acknowledgements This study was in part supported by Health and Labor Science Research Grants for Research on Intractable Diseases and Research on Children and Families from The Ministry of Health, Labor and Welfare of Japan and by a Grant-in-Aid for Scientific Research from the Ministry of Education, Science, Sports and Culture of Japan

References

Adams PD, Afonine PV, Bunkoczi G et al (2010) PHENIX: a comprehensive Python-based system for macromolecular structure solution. Acta Crystallogr D Biol Crystallogr 66:213–221

Berry GT, Fukao T, Mitchell GA et al (2001) Neonatal hypoglycaemia in severe succinyl-CoA: 3-oxoacid CoA-transferase deficiency. J Inherit Metab Dis 24:587–595

Bonnefont JP, Specola NB, Vassault A et al (1990) The fasting test in paediatrics: application to the diagnosis of pathological hypo- and hyperketotic states. Eur J Pediatr 150:80–85

Cornblath M, Gingell RL, Fleming GA, Tildon JT, Leffler AT, Wapnir RA (1971) A new syndrome of ketoacidosis in infancy. J Pediatr 79:413–418

Emsley P, Cowtan K (2004) Coot: model-building tools for molecular graphics. Acta Crystallogr D Biol Crystallogr 60:2126–2132

Fukao T, Song XQ, Watanabe H et al (1996) Prenatal diagnosis of succinyl-coenzyme A:3-ketoacid coenzyme A transferase deficiency. Prenat Diagn 16:471–474

Fukao T, Song XQ, Mitchell GA et al (1997) Enzymes of ketone body utilization in human tissues: protein and messenger RNA levels of succinyl-coenzyme A (CoA):3-ketoacid CoA transferase and mitochondrial and cytosolic acetoacetyl-CoA thiolases. Pediatr Res 42:498–502

Fukao T, Mitchell GA, Song XQ et al (2000) Succinyl-CoA:3-ketoacid CoA transferase (SCOT): cloning of the human SCOT gene, tertiary structural modeling of the human SCOT monomer, and characterization of three pathogenic mutations. Genomics 68:144–151

Fukao T, Shintaku H, Kusubae R et al (2004) Patients homozygous for the T435N mutation of succinyl-CoA:3-ketoacid CoA Transferase (SCOT) do not show permanent ketosis. Pediatr Res 56:858–863

Fukao T, Sakurai S, Rolland MO et al (2006) A 6-bp deletion at the splice donor site of the first intron resulted in aberrant splicing using a cryptic splice site within exon 1 in a patient with succinyl-CoA: 3-Ketoacid CoA transferase (SCOT) deficiency. Mol Genet Metab 89:280–282

Fukao T, Kursula P, Owen EP, Kondo N (2007) Identification and characterization of a temperature-sensitive R268H mutation in the human succinyl-CoA:3-ketoacid CoA transferase (SCOT) gene. Mol Genet Metab 92:216–221

Kassovska-Bratinova S, Fukao T, Song XQ et al (1996) Succinyl CoA: 3-oxoacid CoA transferase (SCOT): human cDNA cloning, human chromosomal mapping to 5p13, and mutation detection in a SCOT-deficient patient. Am J Hum Genet 59:519–528

Longo N, Fukao T, Singh R et al (2004) Succinyl-CoA:3-ketoacid transferase (SCOT) deficiency in a new patient homozygous for an R217X mutation. J Inherit Metab Dis 27:691–692

Merron S, Akhtar R (2009) Management and communication problems in a patient with succinyl-CoA transferase deficiency in pregnancy and labour. Int J Obstet Anesth 18:280–283

Mitchell GA, Fukao T (2001) Chapter 102. Inborn errors of ketone body catabolism. In: Scriver CR, Beaudet AL, Sly WS, Valle D (eds) Metabolic and molecular bases of inherited disease, 8th edn. McGraw-Hill Inc, New York, pp 2327–2356

Niezen-Koning KE, Wanders RJ, Ruiter JP et al (1997) Succinyl-CoA: acetoacetate transferase deficiency: identification of a new patient with a neonatal onset and review of the literature. Eur J Pediatr 156:870–873

Perez-Cerda C, Merinero B, Sanz P et al (1992) A new case of succinyl-CoA: acetoacetate transferase deficiency. J Inherit Metab Dis 15:371–373

Pretorius CJ, Loy Son GG, Bonnici F, Harley EH (1996) Two siblings with episodic ketoacidosis and decreased activity of succinyl-CoA:3-ketoacid CoA-transferase in cultured fibroblasts. J Inherit Metab Dis 19:296–300

Rolland MO, Guffon N, Mandon G, Divry P (1998) Succinyl-CoA: acetoacetate transferase deficiency. Identification of a new case; prenatal exclusion in three further pregnancies. J Inherit Metab Dis 21:687–688

Sakazaki H, Hirayama K, Murakami S et al (1995) A new Japanese case of succinyl-CoA: 3-ketoacid CoA-transferase deficiency. J Inherit Metab Dis 18:323–325

Saudubray JM, Specola N, Middleton B, Lombes A, Bonnefont JP, Jakobs C, Vassault A, Charpentier C, Day R (1987) Hyperketotic states due to inherited defects of ketolysis. Enzyme 38:80–90

Snyderman SE, Sansaricq C, Middleton B (1998) Succinyl-CoA:3-ketoacid CoA-transferase deficiency. Pediatrics 101:709–711

Song XQ, Fukao T, Yamaguchi S, Miyazawa S, Hashimoto T, Orii T (1994) Molecular cloning and nucleotide sequence of complementary DNA for human hepatic cytosolic acetoacetyl-coenzyme A thiolase. Biochem Biophys Res Commun 201:478–485

Song XQ, Fukao T, Mitchell GA et al (1997) Succinyl-CoA:3-ketoacid coenzyme A transferase (SCOT): development of an antibody to human SCOT and diagnostic use in hereditary SCOT deficiency. Biochim Biophys Acta 1360:151–156

Song XQ, Fukao T, Watanabe H et al (1998) Succinyl-CoA:3-ketoacid CoA transferase (SCOT) deficiency: two pathogenic mutations, V133E and C456F, in Japanese siblings. Hum Mutat 12:83–88

Tildon JT, Cornblath M (1972) Succinyl-CoA: 3-ketoacid CoA-transferase deficiency. A cause for ketoacidosis in infancy. J Clin Invest 51:493–498

Yamada K, Fukao T, Zhang G et al (2007) Single-base substitution at the last nucleotide of exon 6 (c.671G > A), resulting in the skipping of exon 6, and exons 6 and 7 in human succinyl-CoA:3-ketoacid CoA transferase (SCOT) gene. Mol Genet Metab 90:291–297

Tohoku J. Exp. Med., 2010, **221**, 191-195

Carnitine Palmitoyltransferase 2 Deficiency: The Time-Course of Blood and Urinary Acylcarnitine Levels during Initial L-Carnitine Supplementation

Tomohiro Hori,[1] Toshiyuki Fukao,[1,2,3] Hironori Kobayashi,[4] Takahide Teramoto,[1] Masaki Takayanagi,[5] Yuki Hasegawa,[4] Tetsuhiko Yasuno,[6] Seiji Yamaguchi[4] and Naomi Kondo[1]

[1]Department of Pediatrics, Gifu University Graduate School of Medicine, Gifu, Japan
[2]Medical Information Science Division, United Graduate School of Drug Discovery and Medical Information, Gifu University, Gifu, Japan
[3]Clinical Research Division, Nagara Medical Center, Gifu, Japan
[4]Department of Pediatrics, Shimane University School of Medicine, Shimane, Japan
[5]Department of Metabolism, Chiba Children's Hospital, Chiba, Japan
[6]Division of Nephrology and Rheumatology, Department of Internal Medicine, Fukuoka University School of Medicine, Fukuoka, Japan

Carnitine palmitoyltransferase 2 (CPT2) deficiency is one of the most common mitochondrial beta-oxidation defects. A female patient with an infantile form of CPT2 deficiency first presented as having a Reye-like syndrome with hypoglycemic convulsions. Oral L-carnitine supplementation was administered since serum free carnitine level was very low (less than 10 μmol/L), indicating secondary carnitine deficiency. Her serum and urinary acylcarnitine profiles were analyzed successively to evaluate time-course effects of L-carnitine supplementation. After the first two days of L-carnitine supplementation, the serum level of free carnitine was elevated; however, the serum levels of acylcarnitines and the urinary excretion of both free carnitine and acylcarnitines remained low. A peak of the serum free carnitine level was detected on day 5, followed by a peak of acetylcarnitine on day 7, and peaks of long-chain acylcarnitines, such as C16, C18, C18:1 and C18:2 carnitines, on day 9. Thereafter free carnitine became predominant again. These peaks of the serum levels corresponded to urinary excretion peaks of free carnitine, acetylcarnitine, and medium-chain dicarboxylic carnitines, respectively. It took several days for oral L-carnitine administration to increase the serum carnitine levels, probably because the intracellular stores were depleted. Thereafter, the administration increased the excretion of abnormal acylcarnitines, some of which had accumulated within the tissues. The excretion of medium-chain dicarboxylic carnitines dramatically decreased on day 13, suggesting improvement of tissue acylcarnitine accumulation. These time-course changes in blood and urinary acylcarnitine levels after L-carnitine supplementation support the effectiveness of L-carnitine supplementation to CPT2-deficient patients.

Keywords: carnitine palmitoyltransferase 2; CPT2; L-carnitine; acylcarnitine profile; carnitine administration
Tohoku J. Exp. Med., 2010, **221** (3), 191-195.

Carnitine palmitoyltransferase 2 (CPT2) deficiency (EC 2.3.1.21, OMIM 600650) is one of the most common disorders of mitochondrial fatty acid oxidation. CPT2 deficiency has several clinical presentations (Bonnefont et al. 1999). The adult form is characterized by episodes of rhabdomyolysis triggered by prolonged exercise. The infantile form presents as severe attacks of hypoketotic hypoglycemia, occasionally associated with sudden infant death or a Reye-like syndrome (Demaugre et al. 1991; Hug et al. 1991). The most severe kind, the neonatal form, is almost always lethal during the first month of life.

Secondary carnitine deficiency, characterized by low levels of total and free carnitines associated with an increase in the long-chain acylcarnitine fraction, is observed in the infantile form of CPT2-deficient patients (Bonnefont et al. 2004; Longo et al. 2006). Hence, L-carnitine supply might be useful in severe CPT2 deficiencies (Bonnefont et al. 2004), although supplementation with L-carnitine in patients with beta-oxidation defects of long-chain acyl-CoA has long been a matter of controversy (Costa et al. 1998;

Received March 23, 2010; revision accepted for publication May 17, 2010. doi:10.1620/tjem.221.191
Correspondence; Toshiyuki Fukao, M.D., Ph.D., Department of Pediatrics, Gifu University Graduate School of Medicine, Yanagido 1-1, Gifu 501-1194, Japan.
e-mail:toshi-gif@umin.net

Liebig et al. 2006; Primassin et al. 2008).

In this report, we describe a CPT2-deficient patient who presented as having a Reye-like syndrome with secondary carnitine deficiency. We focused on time-dependent changes in the serum and urinary acylcarnitine profiles after intial L-carnitine supplementation.

Clinical Report

The patient, a female, was born to nonconsanguineous Japanese parents. She had been well until 15 months of age when she suddenly had tonic-clonic convulsions at 3:00 a.m. for about 30 minutes and became unconscious. Ten days before the convulsions, she had a cold and was given Cefteram pivoxil (CFTM-PI) for four days. When she arrived at another hospital, she had hypoglycemia (blood glucose 1.1 mmol/L), hepatic dysfunction (AST 85 IU/L, ALT 55 IU/L, LDH 402 IU/L), and mild hyperammoniemia (NH3 84 μmol/L). Urinary ketones were not detected. Brain MRI and cerebrospinal fluid were normal. She was suspected of being affected by a Reye-like syndrome and transferred to Gifu University Hospital.

On admission, her height was 72 cm (−1.5s.d.) and her weight was 10 kg (+0.73s.d.). She had a fever (38.3°C) and exhibited lethargy. Physical examination revealed mild hepatomegaly. A laboratory test showed AST 382 IU/L, ALT 441 IU/L, LDH 557 IU/L, PT 31%, NH3 84 μmol/L, and blood glucose 4.7 mmol/L.

We tentatively diagnosed her as having a Reye-like syndrome and treated her with intravenous glucose. Her consciousness level became clear on the 4th hospital day and she started oral intake of food. An abdominal CT scan still showed hepatomegaly and a fatty liver (20HU) on the 6th hospital day. The finding of cardiac ultrasonography was normal. Urinary organic acid analysis during the hypoglycemic condition showed hypoketotic dicarboxylic aciduria. The initial measurements of serum free carnitine and acyl-

Table 1. Time-course of serum and urinary acylcarnitine levels measured by tandem MS.

	Day	- 1	3	5	7	9	13
Serum (μmol/L)	range						
C0	10 - 55	2.98	12.70	40.75	24.31	18.49	58.22
C2	4 - 60	2.25	3.85	14.87	20.15	8.37	14.8
C8	- 1.0	0.035	0.024	0.088	0.058	0.073	0.10
C8DC	- 0.25	0.035	0.046	0.12	0.89	0.97	0.063
C10	- 0.8	0.055	0.062	0.25	0.12	0.17	0.21
C10DC	- 0.1	0.063	0.12	0.24	0.33	0.53	0.19
C12:1	- 0.2	0.038	0.038	0.18	0.15	0.15	0.091
C12DC	- 0.05	0.053	0.064	0.19	0.14	0.27	0.054
C14:1	- 0.1	0.075	0.16	0.47	0.58	0.68	0.18
C16	- 0.5	1.01	1.29	2.99	4.45	8.07	2.56
C18	- 0.3	0.49	0.65	1.46	1.67	3.07	0.99
C18:1	- 0.46	1.50	1.84	4.21	6.09	10.03	3.62
C18:2	- 0.3	0.46	0.67	1.47	1.43	2.05	0.98
(C16+C18:1)/C2	- 0.36	1.12	0.81	0.48	0.52	2.16	0.42
C total		12.35	26.74	86.07	84.99	67.46	85.52
Urine (μmol/mmol Cr)	range*						
C0	5.67 - 56.09	0.61	1.31	82.33	37.85	45.95	329.15
C2	6.87 - 60.48	0.56	0.02	25.44	128.00	41.83	53.58
C4	0.07 - 0.74	0.31	0.47	0.92	0.47	1.38	2.32
C6	0.04 - 0.48	0.18	0.09	0.21	0.22	0.61	0.23
C6DC		1.25	1.34	1.63	15.69	83.33	2.93
C8	0.05 - 0.39	0.00	0.02	0.33	0.98	1.33	0.62
C8DC		0.25	0.52	0.83	23.90	122.99	1.11
C10	0.03 - 0.36	0.05	0.06	0.11	2.66	1.76	0.12
C10DC		0.11	0.02	0.10	0.75	4.03	0.08
C12DC		0.00	0.02	0.01	0.23	1.52	0.01
C16	0.05 - 1.55	0.04	0.02	0.02	0.18	0.63	0.08
C total		4.75	6.86	122.16	226.51	344.91	408.34

* Reference values for urine acylcarnitines were obtained from data reported by Mueller et al. (2003) (10th - 90th percentile)

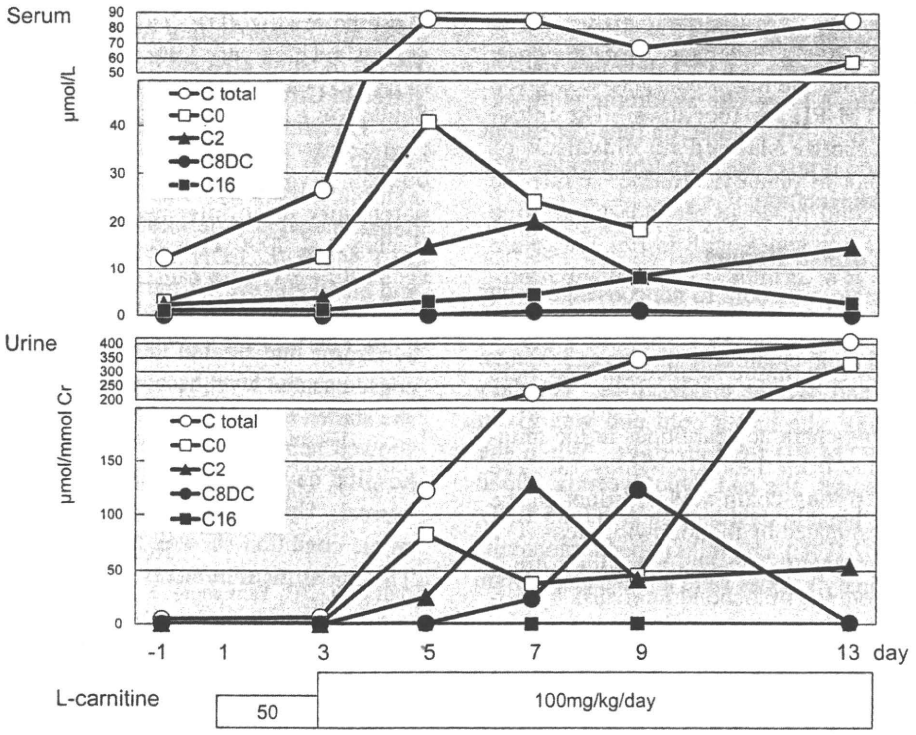

Fig. 1. Time-course of serum and urinary acylcarnitine levels measured by tandem MS. The levels of representative acylcarnitines are shown. The first day of L-carnitine supplementation is designated as day 1. Urinary carnitines were assayed using the first urine in the morning.

carnitine fractions by the enzymatic cycling method were 9.5 and 5.9 μmol/L, respectively. The initial serum acylcarnitine profile (Table 1) showed a very low free carnitine level and relatively high long-chain acylcarnitine levels. This profile was compatible with the secondary carnitine deficiency due to CPT2 or translocase deficiency.

After confirmation of the carnitine deficiency, we supplied her with L-carnitine orally from the 15th hospital day (day 1 in the Table 1 and Fig. 1) at a dose of 50 mg/kg/day for the first two days and 100 mg/kg/day from day 3. Blood and urinary samples were obtained before plus 3, 5, 7, 9 and 13 days after L-carnitine supplementation. During carnitine supplementation, the patient had continuous intravenous glucose infusion of 2.5 mg/kg/min until day 11. We analyzed the serum and urinary acylcarnitines by tandem mass analysis, as previously reported (Mueller et al. 2003; Kobayashi et al. 2007a,b). Table 1 shows details of the analyses. Fig. 1 shows the changing patterns of free carnitine (C0), acetyl-carnitine (C2), C8DC representing medium-chain dicarboxylic acylcarnitines, and C16 representing long-chain acylcarnitines in the serum and urine. Urinary excretion of C0 and acylcarnitines remained at very low levels on day 3. Sequential peaks of free carnitine (day 5), acetylcarnitine (day 7), and long-chain acylcarnitines (day 9) were found in the serum, which corresponded to peaks of free carnitine, acetylcarnitine, and dicarboxylic medium-chain acylcarnitines in the urine.

The fatty liver and hepatomegaly improved as judged by an abdominal CT scan on the 26th hospital day (day 13). Informed consent for a skin biopsy, enzyme assay, and DNA was obtained from the parents. CPT2 activity in the patient's fibroblasts was 0.18 nmol/min/mg of protein (3 controls; 0.82, 1.27, and 1.26 nmol/min/mg of protein), confirming the diagnosis of CPT2 deficiency.

Now the patient is 4 years of age. After carnitine supplementation, she did not experience hypoglycemia at all. She is being treated with 1,000 mg L-carnitine/day (current body weight 19.8 kg). Her growth and development are within normal ranges. She had some rhabdomyolysis attacks (the highest CK recorded was 16,769 IU/L) during a febrile illness even after L-carnitine supplementation.

Discussion

The diagnosis of CPT2 deficiency was first suspected by the data on urinary organic acid analysis and acylcarnitine analysis and was confirmed by enzyme assay using fibroblasts. Our patient is a compound heterozygote of a previously reported E174K mutation from the father and an unknown mutation from the mother which was not detected by exon sequencing. According to an in vitro expression analysis of mutant CPT2 cDNAs carrying E174K, the mutant E174K protein was present as much as a wild type protein and retained 10% residual CPT2 activity (Wataya et al. 1998). This "mild" mutation from the father, together with possible null mutation from the mother, may result in an infantile form of CPT2 deficiency.

Initially, she developed secondary carnitine deficiency. Chronic administration of pivalate-conjugated antibiotics is